

A Numerical Scheme for the Quantum Fokker-Planck-Landau Equation Efficient in the Fluid Regime

Jingwei Hu¹, Shi Jin^{2,3,*} and Bokai Yan²

¹ *Institute for Computational Engineering and Sciences (ICES), The University of Texas at Austin, 1 University Station C0200, Austin, TX 78712, USA.*

² *Department of Mathematics, University of Wisconsin-Madison, 480 Lincoln Drive, Madison, WI 53706, USA.*

³ *Department of Mathematics and Institute of Natural Sciences, Shanghai Jiao Tong University, Shanghai 200240, China.*

Received 22 April 2011; Accepted (in revised version) 9 January 2012

Communicated by Pingwen Zhang

Available online 4 June 2012

Abstract. We construct an efficient numerical scheme for the quantum Fokker-Planck-Landau (FPL) equation that works uniformly from kinetic to fluid regimes. Such a scheme inevitably needs an implicit discretization of the nonlinear collision operator, which is difficult to invert. Inspired by work [9] we seek a linear operator to penalize the quantum FPL collision term Q_{qFPL} in order to remove the stiffness induced by the small Knudsen number. However, there is no suitable simple quantum operator serving the purpose and for this kind of operators one has to solve the complicated quantum Maxwellians (Bose-Einstein or Fermi-Dirac distribution). In this paper, we propose to penalize Q_{qFPL} by the "classical" linear Fokker-Planck operator. It is based on the observation that the classical Maxwellian, with the temperature replaced by the internal energy, has the same first five moments as the quantum Maxwellian. Numerical results for Bose and Fermi gases are presented to illustrate the efficiency of the scheme in both fluid and kinetic regimes.

AMS subject classifications: 35Q84, 65L04, 76Y05

Key words: Quantum Fokker-Planck-Landau equation, fluid limit, asymptotic-preserving scheme.

*Corresponding author. *Email addresses:* hu@ices.utexas.edu (J. Hu), jin@math.wisc.edu (S. Jin), yan@math.wisc.edu (B. Yan)

1 Introduction

The Fokker-Planck-Landau (FPL) equation is a kinetic model widely used in plasma physics. It describes the time evolution of charged particles in a plasma [21, 22]. When the quantum effects of particles are taken into account, for example, several bosons can occupy the same quantum state while only one fermion can occupy a particular quantum state, one has to use the following so-called quantum Fokker-Planck-Landau equation,

$$\frac{\partial f}{\partial t} + v \cdot \nabla_x f = \frac{1}{\varepsilon} \mathcal{Q}_{qFPL}(f), \quad x \in \Omega \subset \mathbb{R}^{d_x}, \quad v \in \mathbb{R}^{d_v}, \quad (1.1)$$

where $f(t, x, v) \geq 0$ is the phase space distribution function depending on time t , position x and particle velocity v . ε is the Knudsen number which measures the degree of rarefiedness of the particles. It is the ratio of the mean free path and the typical length scale. The quantum collision operator \mathcal{Q}_{qFPL} is given by

$$\mathcal{Q}_{qFPL}(f)(v) = \nabla_v \cdot \int_{\mathbb{R}^{d_v}} A(v - v_*) [f_*(1 \pm \theta_0 f_*) \nabla_v f - f(1 \pm \theta_0 f) \nabla_{v_*} f_*] dv_* \quad (1.2)$$

with $f = f(t, x, v)$ and $f_* = f(t, x, v_*)$. $A(z) = \Psi(|z|)\Pi(z)$ is a $d_v \times d_v$ semi-positive definite matrix and $\Pi(z)$ is the orthogonal projection onto the space orthogonal to z ,

$$\Pi(z) = I - \frac{z \otimes z}{|z|^2}, \quad I \text{ is the identity matrix.} \quad (1.3)$$

For inverse-power law interactions, $\Psi(|z|) = |z|^{\gamma+2}$ with $-3 \leq \gamma \leq 1$. The case $\gamma = -3$ refers to the Coulomb potential which is of primary importance in plasma applications. The parameter $\theta_0 = \hbar^{d_v}$, where \hbar is the rescaled Planck constant. Here in (1.2) and the sequel, the upper sign will always correspond to the Bose gas (composed of bosons) while the lower sign to the Fermi gas (composed of fermions). For the latter f must also satisfy $f \leq 1/\theta_0$ by the Pauli exclusion principle.

Unlike the classical FPL equation, very few studies have been conducted on the quantum FPL equation. See [7] for a formal derivation from the quantum Boltzmann equation in the grazing collision limit and [23] for a spectral analysis of its linearization near the equilibrium. In the spatially homogeneous setting, the well-posedness and regularity of the solution were established in [1, 5] for Fermi-Dirac particles and the equilibrium states were rigorously determined in [2].

It is well-known that the equilibrium, in this context the quantum Maxwellian \mathcal{M}_q (Bose-Einstein or Fermi-Dirac distribution), is reached when the Knudsen number ε goes to zero. Then we could instead consider the limiting hydrodynamic equations satisfied by the moments of \mathcal{M}_q . However, fluid equations are not adequate for many applications. Very often one has to deal with multiscale phenomena, where the Knudsen number varies between different regimes. Our goal in this paper is to design an efficient numerical scheme for the quantum FPL equation (1.1) that works uniformly for both kinetic and

fluid regimes. The main difficulty arises when ε is very small: the right hand of Eq. (1.1) becomes stiff and due to the diffusive nature of the collision operator explicit schemes are subject to severe stability constraints (require time step $\Delta t = \mathcal{O}(\varepsilon \Delta v^2)$, where Δv is the mesh size in velocity domain). Implicit schemes don't have such a restriction, but a fully nonlinear equation needs to be solved at each time step. Ideally, we would like an implicit scheme that allows larger time step and can be inverted easily.

A class of asymptotic preserving (AP) schemes recently introduced in [9] has successfully resolved this issue for the classical Boltzmann equation. The basic idea is to penalize the collision term with a BGK operator:

$$Q_{CB} = \underbrace{[Q_{CB} - \lambda(\mathcal{M}_c - f)]}_{\text{less stiff}} + \underbrace{\lambda[\mathcal{M}_c - f]}_{\text{stiff}}, \tag{1.4}$$

where Q_{CB} is the classical Boltzmann collision operator. λ is some constant approximation of the spectrum of Q_{CB} . \mathcal{M}_c is the classical Maxwellian given by

$$\mathcal{M}_c = \frac{\rho}{(2\pi T)^{\frac{d_v}{2}}} e^{-\frac{(v-u)^2}{2T}}, \tag{1.5}$$

where ρ is density, u is macro-velocity and T is temperature. Now the first bracket in (1.4) is less stiff than the second one and can be treated explicitly. The second bracket will be discretized implicitly. Using the conservation properties of the BGK operator, this implicit term can actually be handled explicitly [6].

Later, a similar idea was applied to the quantum Boltzmann equation [8] and the classical FPL equation [17]. As the name implies, the quantum FPL equation (1.1) shares the features of both equations: (1) admits the quantum Maxwellian \mathcal{M}_q as the equilibrium state like quantum Boltzmann; (2) becomes the classical FPL when $\theta_0 \rightarrow 0$. Correspondingly, we are facing the numerical challenges from both sides: have to invert a nonlinear 2 by 2 system to define \mathcal{M}_q [8]; the BGK operator is not suitable for penalization since Q_{qFPL} contains diffusion-like terms [17].

In this work, we propose to penalize (1.2) by a "classical" Fokker-Planck (FP) operator:

$$Q_{qFPL} = [Q_{qFPL} - \lambda P_{cFP}(f, \mathcal{M}_c)] + \lambda P_{cFP}(f, \mathcal{M}_c) \tag{1.6}$$

with

$$P_{cFP}(f, \mathcal{M}_c) = \nabla_v \cdot \left(\mathcal{M}_c \nabla_v \left(\frac{f}{\mathcal{M}_c} \right) \right). \tag{1.7}$$

The idea is based on the observation that the classical Maxwellian (1.5), with the temperature replaced by the (quantum) internal energy, has the same first five moments as the quantum Maxwellian. In addition, the classical FP operator (1.7) has good conservation properties and is relatively easy to invert. Thus we arrive at a scheme uniformly stable in ε and avoid computing the complicated quantum Maxwellians. Furthermore, our numerical experiments show that the solution f will converge to \mathcal{M}_q eventually within

an error of $\mathcal{O}(\Delta t)$, no matter what the initial condition is. This guarantees the capturing of the fluid dynamic limit for small Δt in the sense of the asymptotic-preserving schemes [15, 16]. A second order extension is also given.

To implement the above scheme, we need a fast and accurate solver for the quantum FPL operator \mathcal{Q}_{qFPL} . The spectral method introduced in [10, 26] for the classical FPL operator can be easily extended to this case. Even though \mathcal{Q}_{qFPL} is cubic, the fast algorithm still applies, allowing us to reduce the cost from $\mathcal{O}(n^2)$ to $\mathcal{O}(n \log n)$ ($n = N^{d_v}$, N is the number of discretized points in each direction of v). The details of the method are presented in the Appendix.

The rest of the paper is organized as follows. In the next section, we briefly summarize the basic properties of the quantum FPL equation. In Section 3, we describe the numerical schemes. Numerical examples are given in Section 4 to illustrate the asymptotic property and the effectiveness of the scheme in both the kinetic and fluid regimes. Finally we make some concluding remarks in Section 5.

2 The quantum FPL equation and its hydrodynamic limit

In this section we review some basic facts about the quantum FPL equation (1.1). They will be useful to design the numerical scheme.

The weak form of the collision operator (1.2) reads:

$$\int_{\mathbb{R}^{d_v}} \mathcal{Q}_{qFPL}(f) \phi dv = -\frac{1}{2} \iint_{\mathbb{R}^{d_v} \times \mathbb{R}^{d_v}} (\nabla_v \phi - \nabla_{v_*} \phi_*)^T A(v - v_*) f_* f (1 \pm \theta_0 f_*) (1 \pm \theta_0 f) \cdot \left(\frac{1}{1 \pm \theta_0 f} \frac{\nabla_v f}{f} - \frac{1}{1 \pm \theta_0 f_*} \frac{\nabla_{v_*} f_*}{f_*} \right) dv_* dv. \tag{2.1}$$

Then

$$\int_{\mathbb{R}^{d_v}} \mathcal{Q}_{qFPL}(f) dv = \int_{\mathbb{R}^{d_v}} \mathcal{Q}_{qFPL}(f) v dv = \int_{\mathbb{R}^{d_v}} \mathcal{Q}_{qFPL}(f) |v|^2 dv = 0. \tag{2.2}$$

Conservations of mass and momentum are straightforward. Conservation of energy follows from $z^T A(z) = (A(z)z)^T = 0$.

If $\phi = \ln [f / (1 \pm \theta_0 f)]$, one has

$$\begin{aligned} & \int_{\mathbb{R}^{d_v}} \mathcal{Q}_{qFPL}(f) \ln \frac{f}{1 \pm \theta_0 f} dv \\ &= -\frac{1}{2} \iint_{\mathbb{R}^{d_v} \times \mathbb{R}^{d_v}} \left(\frac{1}{1 \pm \theta_0 f} \frac{\nabla_v f}{f} - \frac{1}{1 \pm \theta_0 f_*} \frac{\nabla_{v_*} f_*}{f_*} \right)^T A(v - v_*) \\ & \quad \cdot f_* f (1 \pm \theta_0 f_*) (1 \pm \theta_0 f) \left(\frac{1}{1 \pm \theta_0 f} \frac{\nabla_v f}{f} - \frac{1}{1 \pm \theta_0 f_*} \frac{\nabla_{v_*} f_*}{f_*} \right) dv_* dv \leq 0. \end{aligned} \tag{2.3}$$

This is Boltzmann's H -theorem. The last inequality comes from the semi-positivity of $A(z)$. Moreover,

$$\int_{\mathbb{R}^{d_v}} \mathcal{Q}_{qFPL}(f) \ln \frac{f}{1 \pm \theta_0 f} dv = 0 \iff \mathcal{Q}_{qFPL}(f) = 0 \iff f = \mathcal{M}_q, \tag{2.4}$$

where \mathcal{M}_q is the quantum Maxwellian given by

$$\mathcal{M}_q = \frac{1}{\theta_0} \frac{1}{z^{-1} e^{\frac{(v-u)^2}{2T}} \mp 1}. \tag{2.5}$$

The macroscopic quantity z is called the fugacity: $z = e^{\mu/T}$, μ is the chemical potential (see [13] for more details about the derivation of \mathcal{M}_q). (2.5) is the well-known Bose-Einstein (-) and Fermi-Dirac (+) distributions.

2.1 The hydrodynamic limit

Define the density ρ , macro-velocity u and specific internal energy e as

$$\rho = \int_{\mathbb{R}^{d_v}} f dv, \quad \rho u = \int_{\mathbb{R}^{d_v}} f v dv, \quad \rho e = \frac{1}{2} \int_{\mathbb{R}^{d_v}} f |v-u|^2 dv. \tag{2.6}$$

Then with $f = \mathcal{M}_q$, the first d_v+2 moment equations of (1.1) can be closed and yield the quantum Euler equations:

$$\begin{cases} \frac{\partial \rho}{\partial t} + \nabla_x \cdot (\rho u) = 0, \\ \frac{\partial(\rho u)}{\partial t} + \nabla_x \cdot \left(\rho u \otimes u + \frac{2}{d_v} \rho e I \right) = 0, \\ \frac{\partial}{\partial t} \left(\rho e + \frac{1}{2} \rho u^2 \right) + \nabla_x \cdot \left(\left(\frac{d_v+2}{d_v} \rho e + \frac{1}{2} \rho u^2 \right) u \right) = 0. \end{cases} \tag{2.7}$$

This form is exactly the same as the classical Euler equations. In fact pressure $p = \frac{2}{d_v} \rho e$ holds for both classical and quantum gases. However, the intrinsic equipartition laws are quite different. For classical (monatomic) gas $e = \frac{d_v}{2} T$, while for quantum gas ρ and e are connected with T and z (appeared in the definition of \mathcal{M}_q (2.5)) by a nonlinear 2×2 system:

$$\begin{cases} \rho = \frac{(2\pi T)^{\frac{d_v}{2}}}{\theta_0} Q_{\frac{d_v}{2}}(z), \\ e = \frac{d_v}{2} T \frac{Q_{\frac{d_v+2}{2}}(z)}{Q_{\frac{d_v}{2}}(z)}, \end{cases} \tag{2.8}$$

where $Q_\nu(z)$ denotes the Bose-Einstein function $G_\nu(z)$ and Fermi-Dirac function $F_\nu(z)$ respectively,

$$G_\nu(z) = \frac{1}{\Gamma(\nu)} \int_0^\infty \frac{x^{\nu-1}}{z^{-1} e^x - 1} dx, \quad 0 < z < 1, \quad \nu > 0; \quad z = 1, \quad \nu > 1, \tag{2.9a}$$

$$F_\nu(z) = \frac{1}{\Gamma(\nu)} \int_0^\infty \frac{x^{\nu-1}}{z^{-1} e^x + 1} dx, \quad 0 < z < \infty, \quad \nu > 0, \tag{2.9b}$$

where $\Gamma(\nu) = \int_0^\infty x^{\nu-1} e^{-x} dx$ is the Gamma function.

The physical range of interest for a Bose gas is $0 < z \leq 1$, with $z = 1$ corresponding to the degenerate case (the onset of Bose-Einstein condensation). z could be any positive real number for a Fermi gas and the degenerate case is reached when $z \gg 1$.

For small z , the integrand in (2.9a) and (2.9b) can be expanded in powers of z ,

$$G_\nu(z) = \sum_{n=1}^\infty \frac{z^n}{n^\nu} = z + \frac{z^2}{2^\nu} + \frac{z^3}{3^\nu} + \dots, \tag{2.10a}$$

$$F_\nu(z) = \sum_{n=1}^\infty (-1)^{n+1} \frac{z^n}{n^\nu} = z - \frac{z^2}{2^\nu} + \frac{z^3}{3^\nu} - \dots. \tag{2.10b}$$

Thus both functions behave like z itself for $z \ll 1$ and one recovers the classical limit.

On the other hand, the first equation of (2.8) can be written as

$$Q_{\frac{d\nu}{2}}(z) = \frac{\rho}{(2\pi T)^{\frac{d\nu}{2}}} \theta_0, \tag{2.11}$$

where $\rho / (2\pi T)^{\frac{d\nu}{2}}$ is just the coefficient of the classical Maxwellian and should be an $\mathcal{O}(1)$ quantity. If $\theta_0 \rightarrow 0$, then $Q_{\frac{d\nu}{2}}(z) \rightarrow 0$, which implies $z \rightarrow 0$ by the monotonicity of function Q_ν . This is consistent with the fact that one gets the classical FPL operator in (1.2) by letting $\theta_0 \rightarrow 0$.

3 Numerical schemes

As discussed in Introduction, our goal is to design a numerical scheme for the quantum FPL equation (1.1) that works uniformly for different ε . Inspired by work [9], we seek a suitable operator $P(f, \mathcal{M}_q)$ to penalize Q_{qFPL} . A first-order (in time) scheme should look like:

$$\frac{f^{n+1} - f^n}{\Delta t} + v \cdot \nabla_x f^n = \frac{1}{\varepsilon} [Q_{qFPL}(f^n) - \lambda P(f^n, \mathcal{M}_q^n)] + \frac{\lambda}{\varepsilon} P(f^{n+1}, \mathcal{M}_q^{n+1}). \tag{3.1}$$

To find f^{n+1} , we need to compute \mathcal{M}_q^{n+1} first. This can be accomplished by taking the moments on both sides of (3.1), i.e., multiply by $\phi = (1, v, \frac{1}{2}v^2)^T$ and integrate with respect to v . If $P(f, \mathcal{M}_q)$ preserves mass, momentum and energy, one has

$$\frac{U^{n+1} - U^n}{\Delta t} + \int \phi(v) v \cdot \nabla_x f^n dv = 0, \tag{3.2}$$

where $U = (\rho, \rho u, \rho e + \frac{1}{2} \rho u^2)^T$. Once we get U^{n+1} , \mathcal{M}_q^{n+1} is known, then we go back to (3.1) to compute f^{n+1} .

From the above discussion, we require the operator $P(f, \mathcal{M}_q)$ to satisfy the following conditions:

1. It preserves mass, momentum and energy;
2. It is easy to invert; preferably linear in f ;
3. It contains diffusion-like terms to mimic the structure of \mathcal{Q}_{qFPL} ;
4. It has a unique equilibrium solution: $P(f, \mathcal{M}_q) = 0 \iff f = \mathcal{M}_q$.

Remark 3.1. The last condition is to insure the asymptotic property of the scheme. Simply speaking, if $f^n - \mathcal{M}_q^n = \mathcal{O}(\varepsilon)$, then $\mathcal{Q}_{qFPL}(f^n) = \mathcal{O}(\varepsilon)$, $P(f^n, \mathcal{M}_q^n) = \mathcal{O}(\varepsilon)$. Thus (3.1) implies $P(f^{n+1}, \mathcal{M}_q^{n+1}) = \mathcal{O}(\varepsilon)$, so $f^{n+1} - \mathcal{M}_q^{n+1} = \mathcal{O}(\varepsilon)$. Later we will see this requirement is not necessary if we allow a weaker asymptotic condition.

A similar problem has been thoroughly studied in [17] for the classical FPL equation and the FP operator (1.7) was suggested there as penalization. For the quantum Fokker-Planck-Landau equation, it is very natural to think of an operator $P(f, \mathcal{M}_q)$ that depends on the quantum Maxwellian \mathcal{M}_q and meets all of the above criteria. However, even if one can find such an operator, there is still one difficulty left. In the classical case, if U^{n+1} (conserved quantities) is known then \mathcal{M}_c^{n+1} is readily obtained, but it is not easy to get \mathcal{M}_q^{n+1} . In fact, one has to invert the nonlinear system (2.8) to get z and T in order to define \mathcal{M}_q [8, 13]. In practice this is very expensive (has to be done at every time step and every spatial point). Furthermore, setting a good initial guess for the iterative method is not trivial especially when z is close to the degenerate regime.

Since P_{cFP} works perfectly for the classical FPL equation and \mathcal{M}_q is expensive to invert, motivated by our previous work on the quantum Boltzmann equation [8], we propose P_{cFP} (1.7) as the penalization operator, where

$$\mathcal{M}_c = \rho \left(\frac{d_v}{4\pi e} \right)^{\frac{d_v}{2}} e^{-\frac{d_v}{4e}(v-u)^2}. \tag{3.3}$$

The modification on \mathcal{M}_c is just to replace the temperature T with internal energy e using relation $e = \frac{d_v}{2}T$. The reason is because such defined \mathcal{M}_c has the same first $d_v + 2$ moments as \mathcal{M}_q . Therefore, our scheme for the quantum FPL equation (1.1) reads:

$$\frac{f^{n+1} - f^n}{\Delta t} + v \cdot \nabla_x f^n = \frac{1}{\varepsilon} [\mathcal{Q}_{qFPL}(f^n) - \lambda P_{cFP}(f^n, \mathcal{M}_c^n)] + \frac{\lambda}{\varepsilon} P_{cFP}(f^{n+1}, \mathcal{M}_c^{n+1}). \tag{3.4}$$

The right hand side of (3.4) is still conservative, so one computes \mathcal{M}_c^{n+1} same as before.

It is important to notice that z and T are not present at all in this scheme. If they are desired variables for output, one only needs to convert between ρ , e and z , T through (2.8) at the final time, see [13].

Remark 3.2. In general, one cannot expect $f^{n+1} - \mathcal{M}_q^{n+1} = \mathcal{O}(\varepsilon)$ even if $f^n - \mathcal{M}_q^n = \mathcal{O}(\varepsilon)$ for this new scheme. Since then $\mathcal{Q}_{qFPL}(f^n) = \mathcal{O}(\varepsilon)$ and the other terms on the numerator of the right hand side of (3.4) could be written as, roughly speaking, $\mathcal{O}(f^n - \mathcal{M}_c^n) + \mathcal{O}(f^{n+1} - \mathcal{M}_c^{n+1})$, which is equal to $\mathcal{O}(f^n - \mathcal{M}_q^n) + \mathcal{O}(f^{n+1} - \mathcal{M}_q^{n+1}) + \mathcal{O}(\mathcal{M}_q^{n+1} - \mathcal{M}_q^n) + \mathcal{O}(\mathcal{M}_c^{n+1} - \mathcal{M}_c^n)$. Assuming all the functions are smooth and $\Delta t > \varepsilon$, the last two terms are of $\mathcal{O}(\Delta t)$, this implies $\mathcal{O}(f^{n+1} - \mathcal{M}_q^{n+1}) = \mathcal{O}(\Delta t)$.

Remark 3.3. In [8] when the quantum BGK operator was penalized by the classical BGK operator, we were able to show

$$|f^n - \mathcal{M}_q^n| \leq \alpha^n |f^0 - \mathcal{M}_q^0| + \mathcal{O}(\Delta t), \quad 0 < \alpha < 1. \quad (3.5)$$

Based on this simple analysis, we expect that f will converge to \mathcal{M}_q in (3.4) eventually within an error of $\mathcal{O}(\Delta t)$ for any initial data. The numerical experiments in the next section actually confirm this property for our new scheme, but there is no theoretical justification yet.

At this point, it is beneficial to get a qualitative idea of the differences between classical Maxwellian and quantum Maxwellian, since basically we are replacing \mathcal{M}_q with \mathcal{M}_c in the penalization and still expect f to be driven to \mathcal{M}_q instead of \mathcal{M}_c . As discussed in Section 2, we know that \mathcal{M}_q and \mathcal{M}_c are more or less the same in the classical regime (when $\theta_0 \rightarrow 0$, i.e., $z \ll 1$). What we are really interested in is the behavior of the solution in the quantum regime (when θ_0 is not small, corresponding to $z \sim 1$ for Bose gas and $z \gg 1$ for Fermi gas). Fig. 1 shows the 2-D profile of a typical Bose-Einstein distribution and Fermi-Dirac distribution along with the (classical) gaussian distribution, all obtained with $\rho = T = 1, u = 0$. In the numerical examples of Section 4, we always solve the equation in the quantum regime, where the differences between \mathcal{M}_q and \mathcal{M}_c are evident (θ_0 is not small and may take various values in different examples).

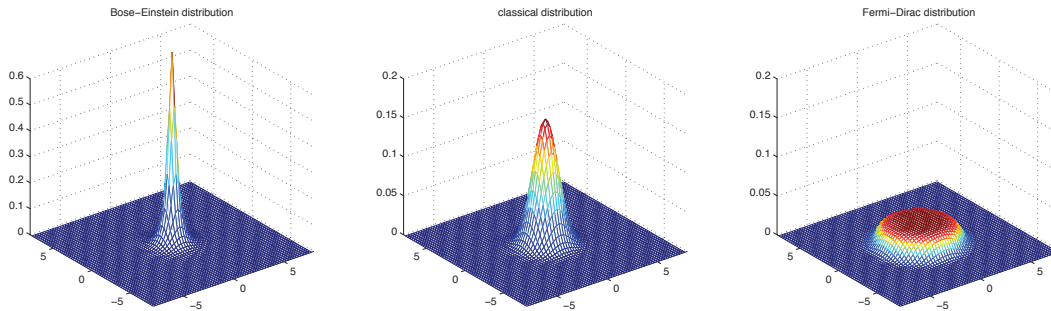


Figure 1: Left: Bose-Einstein distribution ($z=0.9216$); middle: classical Maxwellian ($z \ll 1$); right: Fermi-Dirac distribution ($z=306.8393$).

3.1 The algorithm

We are ready to describe the detailed algorithm.

Given f^n and $U^n = (\rho, \rho u, \rho e + \frac{1}{2} \rho u^2)^n$ at time t^n ,

Step 1. Approximate the transport term $v \cdot \nabla_x f^n$ in (3.2) by a finite volume or finite difference method.

Step 2. Compute U^{n+1} via (3.2) (using any quadrature rule for the integral).

Step 3. Construct \mathcal{M}_c^{n+1} through (3.3).

Step 4. Evaluate $\mathcal{Q}_{qFPL}(f^n)$ by a fast spectral method presented in Appendix A.

Step 5. Solve f^{n+1} by

$$f^{n+1} = \left(I - \frac{\lambda \Delta t}{\varepsilon} P_{cFPL}(\cdot, \mathcal{M}_c^{n+1}) \right)^{-1} \cdot \left(f^n - \Delta t v \cdot \nabla_x f^n + \frac{\Delta t}{\varepsilon} (\mathcal{Q}_{qFPL}(f^n) - \lambda P_{cFPL}(f^n, \mathcal{M}_c^n)) \right). \tag{3.6}$$

The discretization of P_{cFPL} and its inverse can be found in [17], where only a symmetric matrix needs to be inverted by the Conjugate-Gradient method.

A remaining question is how to choose an appropriate λ to approximate the spectrum of \mathcal{Q}_{qFPL} . The form (3.12) indicates a reasonable choice: λ should be the largest eigenvalue of matrix

$$\int_{\mathbb{R}^{d_v}} A(v - v_*) f_*(1 \pm \theta_0 f_*) dv_*. \tag{3.7}$$

Note that the integral is just the convolution of A and $f(1 \pm \theta_0 f)$, which can be obtained via the Fourier transform.

3.2 Discussions on other possible penalty operators

An equivalent form of P_{cFPL} is written as

$$P_{cFPL} = \nabla_v \cdot \left(\nabla_v f + \frac{v-u}{T} f \right). \tag{3.8}$$

This reminds us of the quantum Fokker-Planck or Kaniadakis-Quarati equation [18–20],

$$\frac{\partial f}{\partial t} = \nabla_v \cdot (\nabla_v f + v f(1 \pm \theta_0 f)). \tag{3.9}$$

It was introduced as a simplified model of the full kinetic equation. The well-posedness and long-time asymptotics of the solution were investigated in [3,4]. Recently it was also considered for modeling the Bose-Einstein condensate [28].

For the spatially inhomogeneous case, we define

$$P_{qFPL} = \nabla_v \cdot \left(\nabla_v f + \frac{v-u}{T} f(1 \pm \theta_0 f) \right) \tag{3.10}$$

analogous to its classical counterpart. Let’s check if this operator serves our purpose. It is not hard to see that P_{qFPL} satisfies conditions 3 and 4. However, it is not linear in f which needs more effort to invert than a linear one (although much better than \mathcal{Q}_{qFPL}). Most importantly, P_{qFPL} only preserves mass. Momentum and energy can be bounded [3], but are not strictly conserved.

Another possibility is the following operator:

$$P(f, \mathcal{M}_q) = \nabla_v^2 (f - \mathcal{M}_q). \tag{3.11}$$

This P clearly satisfies conditions 1-4, but it turns out to be a bad choice. We give a simple argument here. The quantum collision operator (1.2) can be rearranged as

$$\nabla_v \cdot \left[\left(\int_{\mathbb{R}^{d_v}} A(v-v_*) f_* (1 \pm \theta_0 f_*) dv_* \right) \nabla_v f - \left(\int_{\mathbb{R}^{d_v}} A(v-v_*) \nabla_{v_*} f_* dv_* \right) f (1 \pm \theta_0 f) \right]. \quad (3.12)$$

On the other hand,

$$\nabla_v^2 (f - \mathcal{M}_q) = \nabla_v \cdot (\nabla_v f - \nabla_v \mathcal{M}_q) = \nabla_v \cdot \left(\nabla_v f + \frac{v-u}{T} \mathcal{M}_q (1 \pm \theta_0 \mathcal{M}_q) \right). \quad (3.13)$$

Comparing (3.12) with (3.13) and (3.10), it is not surprising that the quantum FP operator (3.10) works better than the purely diffusive one (3.11). Similar scenario happens in the classical case, readers are referred to [17] for more explanations and numerical results regarding this issue.

3.3 An extension to second order method

Up to this point we are only dealing with the first order method, in the sense that the numerical accuracy is first order in time, as well as the asymptotic property ($f^n - \mathcal{M}_q^n = \mathcal{O}(\Delta t)$). Here we propose a way to extend scheme (3.4) to second order.

3.3.1 A toy model

We start with the toy model

$$\partial_t f = -\frac{1}{\varepsilon} f. \quad (3.14)$$

A penalty based second order method can be given as,

$$\frac{3f^{n+1} - 4f^n + f^{n-1}}{2\Delta t} = -\frac{1}{\varepsilon} (2f^n - f^{n-1} - \lambda(2f^n - f^{n-1}) + \lambda f^{n+1}). \quad (3.15)$$

Lemma 3.1. *The scheme (3.15) is stable for any ε and Δt if and only if $\lambda \geq 3/4$.*

The proof is straightforward and given in Appendix B.

Remark 3.4. The critical case $\lambda = 3/4$ gives a stable scheme for any nonzero ε . But in the limiting case $\varepsilon = 0$, one of the roots of the characteristic polynomial for (3.15) is -1 . Then (3.15) does not give the right solutions $f^n \rightarrow 0$. In fact, when $\lambda = 3/4$ this method is not L -stable, which is crucial for AP schemes [14].

3.3.2 A second order method for the quantum FPL equation

Now we can give the second order method for the quantum FPL equation:

$$\begin{aligned} \frac{3f^{n+1} - 4f^n + f^{n-1}}{2\Delta t} + v \cdot \nabla_x (2f^n - f^{n-1}) &= \frac{1}{\varepsilon} [2\mathcal{Q}(f^n) - \mathcal{Q}(f^{n-1})] \\ &\quad - \frac{\lambda}{\varepsilon} [2P(f^n, \mathcal{M}_c^n) - P(f^{n-1}, \mathcal{M}_c^{n-1})] + \frac{\lambda}{\varepsilon} P(f^{n+1}, \mathcal{M}_c^{n+1}), \end{aligned} \quad (3.16)$$

where $\mathcal{Q} = \mathcal{Q}_{qFPL}$ is the qFPL operator, $P = P_{cFP}$ is the classical Fokker-Planck operator.

Like the first order method, we don't have any rigorous justification for the quantum FPL equation. But when the scheme is applied to the quantum BGK equation, we can improve the result in [8] with the following proposition.

Proposition 3.1. Suppose $\mathcal{Q}(f)$ in (3.16) is the quantum BGK operator $\mathcal{M}_q - f$ and P is the classical BGK operator $\mathcal{M}_c - f$, then when $\lambda > 3/4$, for any initial data, there exists a constant integer $N > 0$, such that

$$f^n - \mathcal{M}_q^n = \mathcal{O}(\Delta t^2), \quad \text{for any } n \geq N. \quad (3.17)$$

Proof. Under the assumption, the second order method (3.16) reads

$$f^{n+1} - \mathcal{M}_q^{n+1} = \frac{\lambda - 1}{\lambda} (2(f^n - \mathcal{M}_q^n) - (f^{n-1} - \mathcal{M}_q^{n-1})) + A, \quad (3.18)$$

with

$$A = \mathcal{O}(\varepsilon) + \mathcal{O}(\Delta t^2). \quad (3.19)$$

Denote r_1 and r_2 as the two roots of

$$g(r) = r^2 - 2\frac{\lambda - 1}{\lambda}r + \frac{\lambda - 1}{\lambda}. \quad (3.20)$$

One can check that $|r_1| < 1$ and $|r_2| < 1$ under the condition $\lambda > 3/4$.

We write (3.18) as

$$(f^{n+1} - \mathcal{M}_q^{n+1}) - r_2(f^n - \mathcal{M}_q^n) = r_1((f^n - \mathcal{M}_q^n) - r_2(f^{n-1} - \mathcal{M}_q^{n-1})) + A. \quad (3.21)$$

Let $h^n = (f^{n+1} - \mathcal{M}_q^{n+1}) - r_2(f^n - \mathcal{M}_q^n)$, then

$$h^n = r_1 h^{n-1} + A = r_1^2 h^{n-2} + (1 + r_1)A = \dots = r_1^n h^0 + (1 + r_1 + \dots + r_1^{n-1})A. \quad (3.22)$$

Noting the last term is of order $\mathcal{O}(\varepsilon) + \mathcal{O}(\Delta t^2)$ since $|r_1| < 1$.

Take $N > 0$ satisfying $r_1^N = \mathcal{O}(\varepsilon) + \mathcal{O}(\Delta t^2)$, then

$$h^n = \mathcal{O}(\varepsilon) + \mathcal{O}(\Delta t^2), \quad \text{for any } n \geq N.$$

This means

$$f^{n+1} - \mathcal{M}_q^{n+1} = r_2(f^n - \mathcal{M}_q^n) + \mathcal{O}(\varepsilon) + \mathcal{O}(\Delta t^2), \quad \text{for any } n \geq N.$$

With same iterations, one obtains

$$f^{n+1} - \mathcal{M}_q^{n+1} = r_2^{n+1-N}(f^N - \mathcal{M}_q^N) + (1+r_2+\dots+r_2^{n-1})(\mathcal{O}(\varepsilon) + \mathcal{O}(\Delta t^2)).$$

Therefore for n large enough, we have

$$f^{n+1} - \mathcal{M}_q^{n+1} = \mathcal{O}(\varepsilon) + \mathcal{O}(\Delta t^2).$$

This completes the proof. □

This improvement is very promising and deserves more studies. We will show some preliminary results of scheme (3.16) in the next section.

4 Numerical examples

In all the simulations, the velocity space is assumed to be 2-D and the interactions between particles are the Coulomb interactions. A second order finite volume method with slope limiters [24] is applied to the transport part.

Whenever fugacity z and temperature T are needed, we compute them as follows. System (2.8) ($d_v=2$) leads to

$$\frac{Q_1^2(z)}{Q_2(z)} = \frac{\theta_0 \rho}{2\pi e}, \tag{4.1}$$

the left hand side is treated as one function of z and inverted by the secant method. To evaluate the quantum function $Q_\nu(z)$, expansion (2.10a) is used for the Bose-Einstein function. The Fermi-Dirac function is computed by a direct numerical integration. The approach adopted is taken from [27] (Chapter 6.10).

4.1 The spatially homogeneous case

We first check the behavior of the solution in the spatially homogeneous case. Consider the nonequilibrium initial data

$$f_0(v) = \frac{\rho_0}{4\pi T_0} \left(\exp\left(-\frac{|v-u_0|^2}{2T_0}\right) + \exp\left(-\frac{|v+u_0|^2}{2T_0}\right) \right) \tag{4.2}$$

with $\rho_0=1$, $T_0=3/8$ and $u_0=(1,1/2)$. Fig. 2 shows the time evolution of f up to time $t=1.2$ for a Bose gas. Here $\theta_0=9$ which corresponds to $z=0.6635$ (the behavior of the quantum gas is significantly different from that of the classical gas). The Knudsen number $\varepsilon=1e-4$. The computational domain for v is taken as $[-8,8] \times [-8,8]$ with $N=64$ in each direction. Under this condition, an explicit scheme would require $\Delta t = \mathcal{O}(\varepsilon\Delta v^2) \approx 1e-6$,

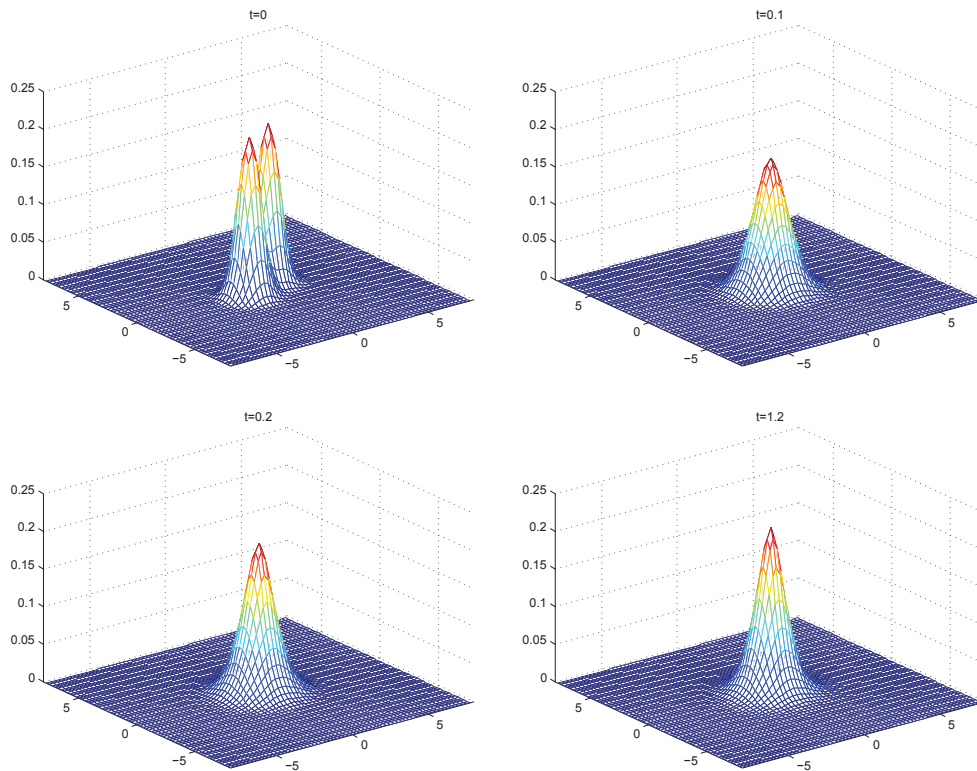


Figure 2: The evolution of f for a Bose gas at times $t = 0, 0.1, 0.2$ and 1.2 . $\theta_0 = 9$. $\varepsilon = 1e-4$. $\Delta t = 0.01$. $v \in [-8,8] \times [-8,8]$ on a 64×64 mesh.

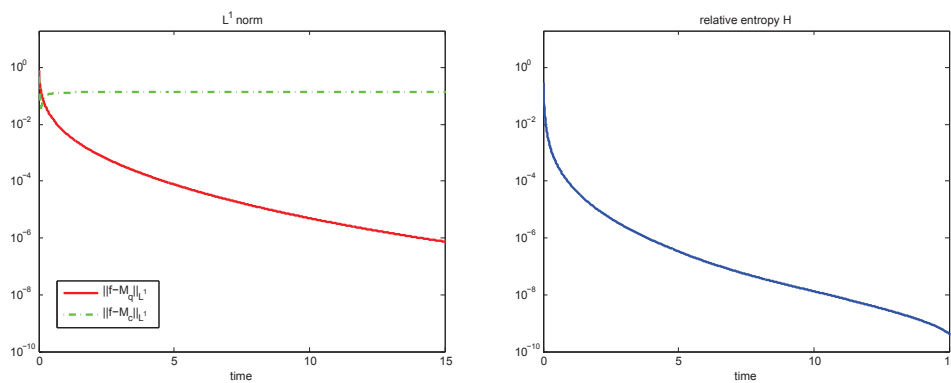


Figure 3: The time evolution of $\|f - \mathcal{M}_q\|_{L^1}$, $\|f - \mathcal{M}_c\|_{L^1}$ (left) and the relative entropy H (right) for a Bose gas. $\theta_0 = 9$. $\varepsilon = 1e-4$. $\Delta t = 0.01$. $v \in [-8,8] \times [-8,8]$ with $N = 64$.

while our scheme (3.4) gives fairly good results with a much coarser time step $\Delta t = 0.01$. Furthermore, Fig. 3 (left) clearly illustrates that the so obtained f is indeed driven to the quantum Maxwellian \mathcal{M}_q rather than classical Maxwellian \mathcal{M}_c . Fig. 3 (right) is the

evolution of the relative entropy H ,

$$H = \int_{\mathbb{R}^{d_v}} \frac{1}{\theta_0} \left[(\theta_0 f) \ln \frac{f}{\mathcal{M}_q} \mp (1 \pm \theta_0 f) \ln \frac{1 \pm \theta_0 f}{1 \pm \theta_0 \mathcal{M}_q} \right] dv. \tag{4.3}$$

By the Boltzmann's H -theorem, this quantity will decay to zero eventually.

4.2 The spatially inhomogeneous case

4.2.1 Asymptotic property

We now numerically verify the asymptotic property of the scheme (3.4) for the spatially inhomogeneous equation. Consider the equilibrium initial data

$$\begin{aligned} \text{(I): } & f_0 = \mathcal{M}_{q_0}, \\ \text{with } & \rho_0 = \frac{\sin(2\pi x) + 2}{3}, \quad u_0 = (0,0), \quad T_0 = \frac{\cos(2\pi x) + 3}{4}, \quad x \in [0,1], \end{aligned} \tag{4.4}$$

and nonequilibrium initial data

$$\begin{aligned} \text{(II): } & f_0 = \frac{\rho_0}{4\pi T_0} \left(\exp\left(-\frac{|v-u_0|^2}{2T_0}\right) + \exp\left(-\frac{|v+u_0|^2}{2T_0}\right) \right), \\ \text{with } & \rho_0 = \frac{\sin(2\pi x) + 2}{3}, \quad u_0 = (0.2,0), \quad T_0 = \frac{\cos(2\pi x) + 3}{4}, \quad x \in [0,1]. \end{aligned} \tag{4.5}$$

We set $\theta_0 = 1$ to get a Bose gas in the quantum regime. The Knudsen number $\varepsilon = 1e-6$. $v \in [-8,8] \times [-8,8]$ with $N=64$. Spatial size $\Delta x=0.01$. $\Delta t=0.0013$ by the CFL condition imposed on the transport part. The periodic boundary condition is used in the x -direction. In Fig. 4, we report the time evolution of $\|f - \mathcal{M}_q\|_{L^1}$ for the equilibrium initial data (I) and nonequilibrium data (II) respectively. As one can see, the distances between f and

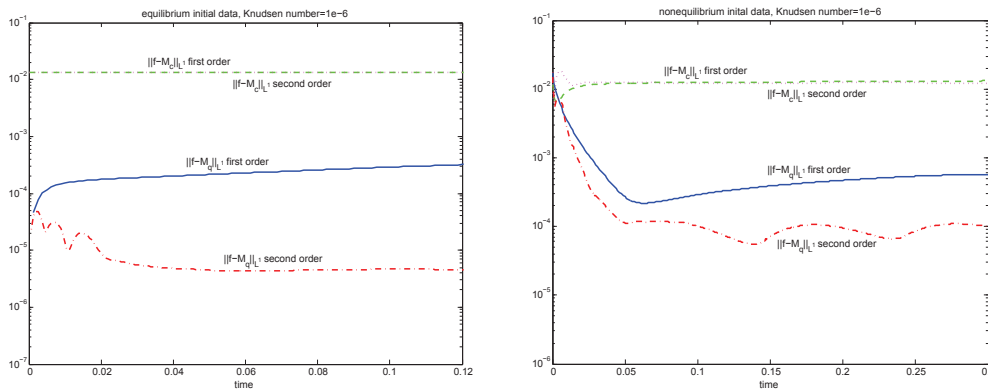


Figure 4: Distances between f and the Maxwellians for a Bose gas. Left: equilibrium initial data (I); right: nonequilibrium initial data (II). $\theta_0 = 1$. $\varepsilon = 1e-6$.

\mathcal{M}_q is about $1e-3 \approx \mathcal{O}(\Delta t)$ as expected. For comparison, we also plot $\|f - \mathcal{M}_c\|_{L^1}$, which is much bigger than $\|f - \mathcal{M}_q\|_{L^1}$.

In the same figure, we also show the results of the second order scheme (3.16): $N=64$, $\Delta x=0.01$, $\Delta t=6.25e-4$. The error is smaller, but we mention that the long term behavior is not satisfactory. A larger N gives better result yet the same increasing trend.

Remark 4.1. The long time behavior is not so satisfactory. This might be due to the lack of well-balanced property for the IMEX type scheme. Consider a conservation equation with a source term

$$\partial_t u + \partial_x f(u) = q(u). \tag{4.6}$$

One can solve it by an IMEX type method

$$\frac{u^{n+1} - u^n}{\Delta t} + \partial_x f(u^n) = q(u^{n+1}). \tag{4.7}$$

However this method is not well balanced in the sense that the stationary solution, i.e., the solution to

$$\partial_x f(u) = q(u) \tag{4.8}$$

is not accurately preserved in the discrete level [11, 12].

This lack of well-balanced property is a typical problem for the long time behavior of AP schemes and deserves further investigation. It is beyond the scope of current work. We leave it for future studies.

4.2.2 A shock tube problem

We next apply our scheme to the 1-D shock tube problem:

$$\begin{cases} (\rho_l, u_l, T_l) = (1, 0, 1), & 0 \leq x \leq 0.5, \\ (\rho_r, u_r, T_r) = (0.125, 0, 0.25), & 0.5 < x \leq 1. \end{cases} \tag{4.9}$$

We adjust $\theta_0 (= 4)$ to get a Fermi gas in the quantum regime ($z_l = 0.8901$, $z_r = 0.3748$). The Knudsen number $\varepsilon = 1e-4$. $v \in [-8, 8] \times [-8, 8]$ with $N = 64$. $\Delta x = 0.01$. $\Delta t = 0.0013$. In this hydrodynamic regime, the solution of the kinetic equation should be close to that of the fluid dynamic equations. So we compare the results of scheme (3.4) with the kinetic scheme (KFVS scheme in [13]) for the quantum Euler equations (2.7). Fig. 5 shows the macroscopic quantities ρ , u , z and T at time $t = 0.2$.

4.2.3 Mixing regime

So far the Knudsen number has been fixed in the numerical simulation and we've seen that our scheme works well in the fluid regime. In the real situation the Knudsen number usually varies between different regimes. The next example is devoted to this kind of problem.

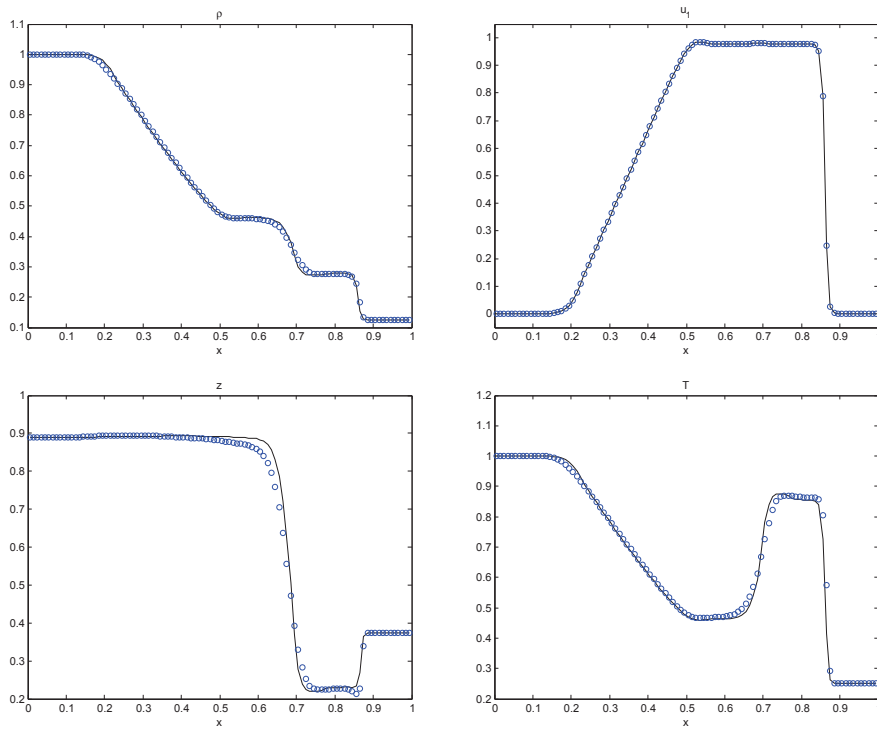


Figure 5: Fermi gas in the fluid regime $\varepsilon=1e-4$. $\theta_0=4$. Density ρ , velocity u_1 , fugacity z and temperature T at $t=0.2$. $v \in [-8,8] \times [-8,8]$ with $N=64$, $\Delta x=0.01$, $\Delta t=0.0013$. \circ : scheme (3.4) for quantum FPL equation; solid line: KFVS scheme for quantum Euler equations.

Assume ε is space-dependent:

$$\varepsilon = \varepsilon_0 + 0.05(\tanh(5 - 10x) + \tanh(5 + 10x)), \quad \varepsilon_0 = 1e-3, \quad x \in [0,1], \quad (4.10)$$

as shown in Fig. 6.

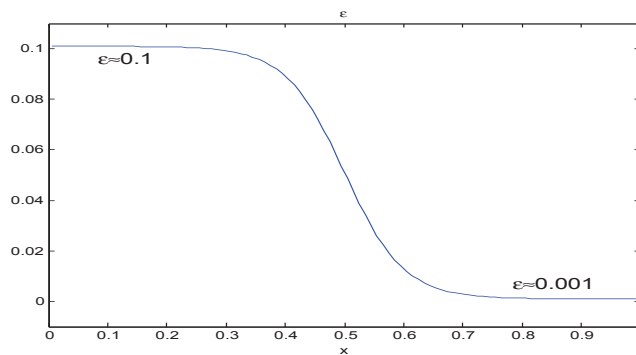


Figure 6: Space-dependent ε .

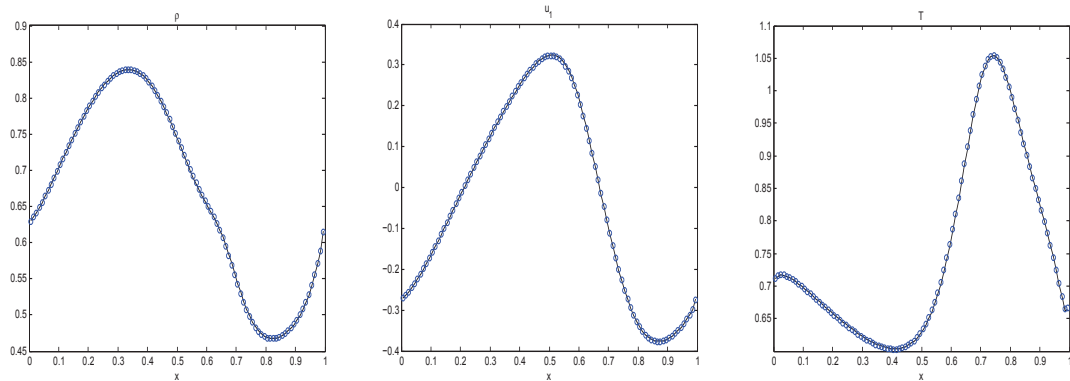


Figure 7: Fermi gas in the mixing regime. $\theta_0 = 2.25$. Density ρ , velocity u_1 and temperature T at $t = 0.2$. $v \in [-8, 8] \times [-8, 8]$ with $N = 64$. $\Delta x = 0.01$. \circ : scheme (3.4) with $\Delta t = 0.0013$; solid line: explicit second-order Runge-Kutta scheme with $\Delta t = 6.7771e - 06$.

We consider a Fermi gas with $\theta_0 = 2.25$ ($z: 0.16 \sim 0.76$) starting from the equilibrium initial data (4.4). Let $v \in [-8, 8] \times [-8, 8]$ with $N = 64$. $\Delta x = 0.01$. $\Delta t = 0.0013$ by the CFL condition, independent of ε . Periodic boundary condition is applied to the x -direction. The macroscopic quantities ρ , u and T at time $t = 0.2$ are plotted in Fig. 7. The reference solution is computed by an explicit second-order Runge-Kutta method with a much smaller time step $\Delta t = 6.7771e - 06$. All the results agree pretty well which demonstrates that the scheme is also reliable for problems with mixing scales.

5 Conclusions

An efficient numerical scheme was constructed for the quantum Fokker-Planck-Landau equation (1.1) that works uniformly for different Knudsen numbers. The main idea is to penalize the quantum collision operator \mathcal{Q}_{qFPL} (1.2) by the "classical" Fokker-Planck operator P_{cFP} (1.7), with the temperature T replaced by internal energy e in the classical Maxwellian \mathcal{M}_c . The implicit P_{cFP} term can be easily inverted while \mathcal{Q}_{qFPL} is much more complex to invert. A remarkable feature of the scheme is that the numerical solution f is still driven to the quantum Maxwellian rather than \mathcal{M}_c under the fluid regime. We also developed a fast spectral method for the collision operator \mathcal{Q}_{qFPL} following its classical counterpart.

Appendix

A A fast spectral method for the quantum FPL collision operator

In this Appendix, we outline the fast spectral method for evaluating the quantum FPL collision operator (1.2). It is an extension of the spectral method in [10, 26] for the classical FPL operator.

In order to develop a spectral approximation, we restrict the function f on the cube $\mathcal{D}_T = [-T, T]^{d_v}$ and extend it periodically to the whole domain. T is chosen such that $T = 2R$, where $B(0, R)$ is the compact support of f [25]. We can then write the operator (1.2) as ([26])

$$\mathcal{Q}_{qFPL}(f)(v) = \nabla_v \cdot \int_{B(0, 2R)} A(g) [h(v+g)\nabla_v f(v) - h(v)\nabla_g f(v+g)] dg, \tag{A.1}$$

where

$$A(g) = |g|^{\gamma+2} \left(I - \frac{gg^T}{|g|^2} \right), \quad h(v) = f(v)(1 \pm \theta_0 f(v)).$$

Now f and h are approximated by truncated Fourier series,

$$f(v) \approx \sum_{k=-\frac{N}{2}}^{\frac{N}{2}-1} \hat{f}_k e^{i\frac{\pi}{T}k \cdot v}, \quad \hat{f}_k = \frac{1}{(2T)^{d_v}} \int_{\mathcal{D}_T} f(v) e^{-i\frac{\pi}{T}k \cdot v} dv, \tag{A.2a}$$

$$h(v) \approx \sum_{k=-\frac{N}{2}}^{\frac{N}{2}-1} \hat{h}_k e^{i\frac{\pi}{T}k \cdot v}, \quad \hat{h}_k = \frac{1}{(2T)^{d_v}} \int_{\mathcal{D}_T} h(v) e^{-i\frac{\pi}{T}k \cdot v} dv. \tag{A.2b}$$

Plugging them into (A.1), one can get the k -th mode of $\hat{\mathcal{Q}}_{qFPL}$,

$$\begin{aligned} \hat{\mathcal{Q}}_{qFPL, k} = & -\frac{\pi^2}{T^2} \sum_{\substack{l, m=-\frac{N}{2} \\ l+m=k}}^{\frac{N}{2}-1} \left[\int_{B(0, 2R)} |g|^{\gamma+2} [l(l+m) - (l \cdot \mu)((l+m) \cdot \mu)] e^{i\frac{\pi}{T}m \cdot s} dg \hat{f}_l \hat{h}_m \right. \\ & \left. - \int_{B(0, 2R)} |g|^{\gamma+2} [m(l+m) - (m \cdot \mu)((l+m) \cdot \mu)] e^{i\frac{\pi}{T}m \cdot s} dg \hat{f}_m \hat{h}_l \right], \end{aligned} \tag{A.3}$$

where $\mu = g/|g|$. Following [26], we define

$$F(m) = \int_{B(0, 2R)} |g|^{\gamma+2} e^{i\frac{\pi}{T}m \cdot s} dg, \tag{A.4a}$$

$$I_{pq}(m) = \int_{B(0, 2R)} |g|^\gamma g_p g_q e^{i\frac{\pi}{T}m \cdot s} dg, \quad p, q = 1, \dots, d_v. \tag{A.4b}$$

Then (A.3) can be recast as

$$\begin{aligned} \hat{\mathcal{Q}}_{qFPL, k} = & -\frac{\pi^2}{T^2} \sum_{\substack{l, m=-\frac{N}{2} \\ l+m=k}}^{\frac{N}{2}-1} \left[l^2 F(m) \hat{f}_l \hat{h}_m + m l F(m) \hat{f}_l \hat{h}_m - m^2 F(m) \hat{f}_m \hat{h}_l - m l F(m) \hat{f}_m \hat{h}_l \right. \\ & - \sum_{p, q=1}^{d_v} l_p l_q I_{pq}(m) \hat{f}_l \hat{h}_m - \sum_{p, q=1}^{d_v} l_p m_q I_{pq}(m) \hat{f}_l \hat{h}_m \\ & \left. + \sum_{p, q=1}^{d_v} m_p l_q I_{pq}(m) \hat{f}_m \hat{h}_l + \sum_{p, q=1}^{d_v} m_p m_q I_{pq}(m) \hat{f}_m \hat{h}_l \right]. \end{aligned} \tag{A.5}$$

Every term in (A.5) is a convolution, which can be computed by the Fast Fourier Transform in $\mathcal{O}(n \log(n))$ operations, where $n = N^{d_v}$ is the total points in the velocity space.

As for $F(m)$ and $I_{pq}(m)$, we precalculated them according to the formulas given in [26]. In the 2-D case, a factor $(T/\pi)^{\gamma+4}$ needs to be multiplied to their results since we are dealing with the arbitrary domain \mathcal{D}_T .

B The stability of the second order method for the toy model

Here we prove Lemma 3.1.

Proof. Eq. (3.15) gives

$$f^{n+1} + \frac{-4(1 + \frac{\Delta t}{\varepsilon}(\lambda - 1))}{3 + \frac{2\Delta t}{\varepsilon}\lambda} f^n + \frac{1 + \frac{2\Delta t}{\varepsilon}(\lambda - 1)}{3 + \frac{2\Delta t}{\varepsilon}\lambda} f^{n-1} = 0.$$

Let

$$g(r) = \left(3 + \frac{2\Delta t}{\varepsilon}\lambda\right)r^2 - 4\left(1 + \frac{\Delta t}{\varepsilon}(\lambda - 1)\right)r + \left(1 + \frac{2\Delta t}{\varepsilon}(\lambda - 1)\right). \tag{B.1}$$

Suppose the two roots of $g(r)$ are r_1 and r_2 . If $r_1 \neq r_2$, the solution $\{f^n\}$ is given by

$$f^n = c_1 r_1^n + c_2 r_2^n, \tag{B.2}$$

where c_1 and c_2 are determined by f^0 and f^1 . If $r_1 = r_2$, the solution $\{f^n\}$ is given by

$$f^n = c_1 r_1^n + c_2 n r_1^n. \tag{B.3}$$

Therefore the stability of method (3.15) is equivalent to the condition that $|r_1| < 1$, $|r_2| < 1$.

Note that the parabola $g(r)$ opens upward and

$$g(1) = 2\frac{\Delta t}{\varepsilon} > 0.$$

Case 1. $\lambda \geq 1$. Note that

$$\begin{aligned} g(0) &= 1 + \frac{2\Delta t}{\varepsilon}(\lambda - 1) > 0, \\ 0 &< \frac{r_1 + r_2}{2} = \frac{2(1 + \frac{\Delta t}{\varepsilon}(\lambda - 1))}{3 + \frac{2\Delta t}{\varepsilon}\lambda} < 1, \\ 0 &< r_1 r_2 = \frac{1 + \frac{2\Delta t}{\varepsilon}(\lambda - 1)}{3 + \frac{2\Delta t}{\varepsilon}\lambda} < 1. \end{aligned}$$

- Case 1.1, r_1 and r_2 are real. Then $0 < r_1 < 1$, $0 < r_2 < 1$.
- Case 1.2, r_1 and r_2 are not real. Then $|r_1| = |r_2| = \sqrt{r_1 r_2} < 1$.

Case 2. $\frac{3}{4} \leq \lambda < 1$. Note that

$$g(-1) = 8 + \frac{\Delta t}{\varepsilon}(8\lambda - 6) > 0,$$

$$-1 < \frac{r_1 + r_2}{2} = \frac{2(1 + \frac{\Delta t}{\varepsilon}(\lambda - 1))}{3 + \frac{2\Delta t}{\varepsilon}\lambda} < 1.$$

- Case 2.1, r_1 and r_2 are real. Then $-1 < r_1 < 1$, $-1 < r_2 < 1$.
- Case 2.2, r_1 and r_2 are not real. Then $g(0) > 0$, hence

$$0 < \frac{g(0)}{3 + \frac{2\Delta t}{\varepsilon}\lambda} = \frac{1 + \frac{2\Delta t}{\varepsilon}(\lambda - 1)}{3 + \frac{2\Delta t}{\varepsilon}\lambda} < 1,$$

i.e., $0 < r_1 r_2 < 1$. Then $|r_1| = |r_2| = \sqrt{r_1 r_2} < 1$.

We have shown that the scheme is stable if $\lambda \geq \frac{3}{4}$.

If $\lambda < \frac{3}{4}$, with ε small enough,

$$g(-1) = 8 + \frac{\Delta t}{\varepsilon}(8\lambda - 6) < 0.$$

Since $g(r)$ is a parabola that opens upward, there must be a root $r_1 < -1$, which makes the scheme unstable. \square

Acknowledgments

This work was partially supported by NSF grant DMS-0608720 and NSF FRG grant DMS-0757285. S. Jin was also supported by a Van Vleck Distinguished Research Prize and a Vilas Associate Award from the University of Wisconsin-Madison.

References

- [1] V. Bagland, Well-posedness for the spatially homogeneous Landau-Fermi-Dirac equation for hard potentials, Proc. R. Soc. Edinburgh Ser. A, 134 (2004), 415–447.
- [2] V. Bagland and M. Lemou, Equilibrium states for the Landau-Fermi-Dirac equation, Banach Center Publ., 66 (2004), 29–37.
- [3] J. A. Carrillo, P. Laurençot and J. Rosado, Fermi-Dirac-Fokker-Planck equation: well posedness and long-time asymptotics, J. Differ. Equ., 247 (2009), 2209–2234.
- [4] J. A. Carrillo, J. Rosado and F. Salvarani, 1D nonlinear Fokker-Planck equations for fermions and bosons, Appl. Math. Lett., 21 (2008), 148–154.
- [5] Y. Chen, Analytic regularity for solutions of the spatially homogeneous Landau-Fermi-Dirac equation for hard potentials, Kinet. Relat. Models, 3 (2010), 645–667.

- [6] F. Coron and B. Perthame, Numerical passage from kinetic to fluid equations, *SIAM J. Numer. Anal.*, 28 (1991), 26–42.
- [7] P. Danielewicz, Nonrelativistic and relativistic Landau/Fokker-Planck equation for arbitrary statistics, *Phys. A*, 100 (1980), 167–182.
- [8] F. Filbet, J. W. Hu and S. Jin, A numerical scheme for the quantum Boltzmann equation with stiff collision terms, *ESAIM: M2AN*, 46 (2012), 443–463.
- [9] F. Filbet and S. Jin, A class of asymptotic-preserving schemes for kinetic equations and related problems with stiff sources, *J. Comput. Phys.*, 229 (2010), 7625–7648.
- [10] F. Filbet and L. Pareschi, A numerical method for the accurate solution of the Fokker-Planck-Landau equation in the nonhomogeneous case, *J. Comput. Phys.*, 179 (2002), 1–26.
- [11] L. Gosse and G. Toscani, Space localization and well-balanced schemes for discrete kinetic models in diffusive regimes, *SIAM J. Numer. Anal.*, 41 (2004), 641–658.
- [12] J. M. Greenberg, A. Y. LeRoux, R. Baraille and A. Noussair, Analysis and approximation of conservation laws with source terms, *SIAM J. Numer. Anal.*, 34 (1997), 1980–2007.
- [13] J. W. Hu and S. Jin, On kinetic flux vector splitting schemes for quantum Euler equations, *Kinet. Relat. Models*, 4 (2011), 517–530.
- [14] S. Jin, Runge-Kutta methods for hyperbolic conservation laws with stiff relaxation terms, *J. Comput. Phys.*, 122 (1995), 51–67.
- [15] S. Jin, Efficient asymptotic-preserving (AP) schemes for some multiscale kinetic equations, *SIAM J. Sci. Comput.*, 21 (1999), 441–454.
- [16] S. Jin, Asymptotic preserving (AP) schemes for multiscale kinetic and hyperbolic equations: a review (Lecture Notes for Summer School on “Methods and Models of Kinetic Theory”, Porto Ercole, June 2010). *Rivista di Matematica della Università di Parma*, to appear.
- [17] S. Jin and B. Yan, A class of asymptotic-preserving schemes for the Fokker-Planck-Landau equation, *J. Comput. Phys.*, 230 (2011), 6420–6437.
- [18] G. Kaniadakis, Generalized Boltzmann equation describing the dynamics of bosons and fermions, *Phys. Lett. A*, 203 (1995), 229–234.
- [19] G. Kaniadakis and P. Quarati, Kinetic equation for classical particles obeying an exclusion principle, *Phys. Rev. E*, 48 (1993), 4263–4270.
- [20] G. Kaniadakis and P. Quarati, Classical model of bosons and fermions, *Phys. Rev. E*, 49 (1994), 5103–5110.
- [21] L. D. Landau, Die kinetische Gleichung für den Fall Coulombscher Wechselwirkung, *Phys. Z. Sowjetunion*, 10 (1936), 154–164.
- [22] L. D. Landau, The kinetic equation in the case of Coulomb interaction. *Zh. Eksper. I Teoret. Fiz.*, 7 (1937), 203–209.
- [23] M. Lemou, Linearized quantum and relativistic Fokker-Planck-Landau equations, *Math. Meth. Appl. Sci.*, 23 (2000), 1093–1119.
- [24] R. J. LeVeque, *Numerical Methods for Conservation Laws*, Birkhäuser Verlag, Basel, second edition, 1992.
- [25] L. Pareschi and G. Russo, Numerical solution of the Boltzmann equation I: spectrally accurate approximation of the collision operator, *SIAM J. Numer. Anal.*, 37 (2000), 1217–1245.
- [26] L. Pareschi, G. Russo and G. Toscani, Fast spectral methods for the Fokker-Planck-Landau collision operator, *J. Comput. Phys.*, 165 (2000), 216–236.
- [27] W. H. Press, S. A. Teukolsky, W. T. Vetterling and B. P. Flannery, *Numerical Recipes: The Art of Scientific Computing*, Cambridge University Press, Cambridge, third edition, 2007.
- [28] G. Toscani, Finite time blow up in Kaniadakis-Quarati model of Bose-Einstein particles, *Commun. Part. Diff. Eqns.*, 37 (2012), 77–87.